

**DSCC2015-9913****OBSERVER-BASED DIAGNOSTIC SCHEME FOR LITHIUM-ION BATTERIES**

**Zoleikha Abdollahi Biron**  
Clemson University  
Greenville, SC-29607, USA  
[zabdoll@clemson.edu](mailto:zabdoll@clemson.edu)

**Pierluigi Pisu**  
Clemson University  
Greenville, SC-29607, USA  
[pisup@clemson.edu](mailto:pisup@clemson.edu)

**Beshah Ayalew**  
Clemson University  
Greenville, SC-29607, USA  
[beshah@clemson.edu](mailto:beshah@clemson.edu)

**ABSTRACT**

This paper presents an observer-based fault diagnosis approach for Lithium-ion batteries. This method detects and isolates five fault types, which include sensor faults in current, voltage and temperature sensors, failure in fan actuator and a fault in battery State-of-Charge (SOC) dynamics. Current, voltage and temperature of the battery are taken as the only available measurements and a Kalman filter and a sliding mode observer are constructed. Three residuals derived from a combination of these observers generate fault signatures that are used to detect and isolate the sensor, actuator and SOC faults in the system. Simulation results show the effectiveness of the approach.

**INTRODUCTION**

Lithium-ion batteries provide higher power and energy densities than other existing batteries such as Ni-MH and Ni-Cd. Hence, they are widely used in various applications such as the PHEV/EV applications [1-2]. Long-life, high capacity, absence of memory effect and high energy to weight ratio are some of Li-ion batteries' characteristics that make them suitable energy storage for a range of applications [3]. Failures in Li-ion batteries can lead to damages, repairing costs and even serious consequences such as explosion due to short-circuiting and overheating. Some of these faults, if not detected or isolated, may cause to catastrophic failures. Comprehensive reviews of the different failure mechanisms can be found in [4] and [5]. Since Li-ion batteries have come in to popular use, fault diagnosis and health monitoring for Li-ion batteries have gathered much attention in the research community in recent years to enhance safety and reliability of these batteries for diverse applications [6-8].

Li-ion battery dynamic behavior is a result of complex electrochemical processes, which have proven difficult to reproduce in a computationally expedient battery model. Most of the existing approaches in the literature use electrical equivalent circuit or electrochemical models for battery modeling. The electrochemical model can capture the electrochemical

phenomena of the battery; it can be computationally too expensive for fault diagnosis purposes while the electrical equivalent circuit can be relatively simple. In equivalent circuit model several RC pairs can be added to characterize system's dynamics. In this paper, we use an equivalent circuit coupled with a thermal model to describe Li-ion battery dynamics.

The scarcity of available measurements of Li-ion batteries, which are basically limited to current, voltage and body-temperature, make the fault diagnosis problem challenging. Several existing methods including the extended Kalman filter, autoregressive moving average model and fuzzy logic, have been used to detect different faults [7]. In [8], a nonlinear fault detection and isolation scheme has been developed using an equivalent circuit model to detect sensor and actuation faults. An observer based fault diagnostic approach used in [9] to estimate and detect some internal electrochemical faults. Ablay in [10], has used Kalman filter to detect and isolate sensor faults and unexpected resistance deviation.

This paper combines a Kalman filter observer with nonlinear sliding mode observer to detect and isolate the faults and disturbance in the Li-ion battery. The rest of the paper is organized as follows. Section II presents modeling of the battery. Fault diagnosis process containing two observer designs is described in section III. In Section IV, we provide threshold setting method while simulation results with realistic current data are given and discussed in Section V.

**SYSTEM MODELING**

Lithium-ion batteries can be modeled in different ways such as: electrochemical models [11-13], equivalent circuit models [14-16] and data driven models [18-19]. Here, we have considered an equivalent circuit for modeling and simulating the Li-ion battery. The equivalent circuit mainly consists of three fundamental parts: electrical model, thermal model and battery SOC model.

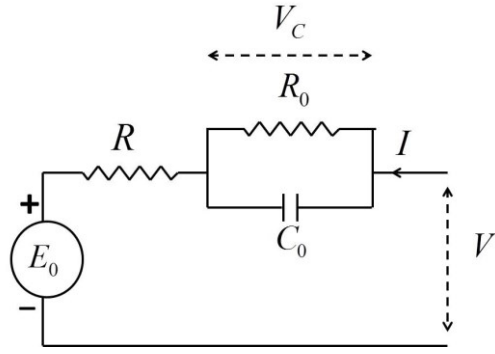


**Figure 1:** Thevenin equivalent model for the battery

### A. Electrical model

One of the most common modeling methods for battery modeling is a simple first-order Thevenin equivalent model. In this study a Thevenin equivalent model with time varying parameters has been considered to model the electrical characteristics of the battery with sufficient accuracy. Fig.1 shows the first-order Thevenin equivalent model.

Dynamics of the first-order electric model can be described via the following equations:

$$\frac{dV_c}{dt} = -\frac{V_c}{R_0 C_0} + \frac{I}{C_0} \quad (1)$$

$$V = E_0 - IR - V_c \quad (2)$$

where  $E_0$  presents the open-circuit voltage,  $V$  and  $I$  show the battery terminal voltage and current, respectively,  $C_0$  presents capacitance and finally,  $R$  and  $R_0$  stands for the internal and over-voltage resistances. It is worth mentioning that  $R_0$  and  $R$  are nonlinear functions of battery state of charge (SOC) and battery temperature.

$$R_0 = K_{10} + K_{20} SOC \cdot T_{body} \quad (3)$$

$$R_1 = K_{11} + K_{21} SOC \cdot T_{body} \quad (4)$$

where  $T_{body}$  is the battery body temperature (in °C) and all  $K_{10}$ ,  $K_{20}$ ,  $K_{11}$  and  $K_{21}$  are different constant values for charging and discharging conditions.

### B. Thermal model

A suitable thermal model is important for analyzing the thermal behavior of the battery. Battery temperature directly relates to heat transfer mechanism, which can be modeled with power loss in the electrical model resistors ( $R_0$  and  $R$ ) and heat exchange of battery with its surrounding environment. Therefore, battery temperature dynamics can be expressed by (5). This equation shows that the thermal model of the battery is coupled to electrical model and depends on time varying parameters in the electrical model such as resistors.

$$m_c \frac{dT_{body}}{dt} = I^2(R + R_0) - hA (T_{body} - T_{amb}) \quad (5)$$

where  $m_c$  (in  $J/^\circ C$ ) is the effective heat capacity per cell,  $hA$  (in  $J/^\circ C$ ) is the effective heat transfer per cell,  $T_{amb}$  (in °C) is the ambient temperature. The effective heat transfer can be considered as function of fan setting based on the following equation:

$$hA = hA_0 \left(1 + \frac{f_s}{2}\right) \quad , \quad hA_0 = 0.07(J/^\circ C) \quad (6)$$

where  $f_s$  presents the fan setting depending on the temperature:

$$\begin{cases} f_s = 0 & \text{off mode} \\ f_s = 1 & \text{if } T \geq 30^\circ C \\ f_s = 2 & \text{if } T \geq 40^\circ C \\ f_s = 3 & \text{if } T \geq 45^\circ C \end{cases} \quad (7)$$

### C. State of Charge (SOC)

Evolution of the SOC can be described with the following equations;

$$\frac{dSOC}{dt} = -\frac{I}{C_0} \quad (8)$$

$$SOC = SOC_0 - \int_{t_0}^t \frac{I}{C} \quad (9)$$

where  $C$  is the capacity of the battery in (A.h)

## FAULT DIAGNOSIS SCHEME

Since Lithium-ion batteries are sealed packs, we assume that the only available measurements are of the voltage, current and temperature of the battery. Hence, estimating inherent parameters and the system's states by designing observers is a practical way for health monitoring and fault diagnosis in this nonlinear system. As it is mentioned in the last section, parameters of the equivalent electro-thermal model are time varying and depend on the battery's inherent characteristics such as SOC and battery temperature. This nonlinearity and time-varying parameters make the battery a complex system for fault diagnosis. In this study, fault in body temperature, voltage and current sensors have been considered in addition to a bias disturbance or fault on the SOC dynamics and an actuator (cooling fan) failure in the cooling system. The faults and disturbance are applied as individual fault scenario to the battery's simulator designed in SIMULINK/MATLAB based on nonlinear dynamics equations (1)-(9).

### D. Kalman-filter Observer

In this part, a Kalman filter approach has been designed to estimate SOC and  $V_c$  as two states of the system while considering the battery voltage as the measurable output. Dynamics of the plant and observer can be written as the following sets of equations (10) and (11), respectively.

$$\begin{cases} \frac{dV_c}{dt} = -\frac{V_c}{R_0 C_0} + \frac{I}{C_0} \\ \frac{dSOC}{dt} = -\frac{I}{C} \end{cases} \quad (10)$$

Dynamic of the observer can be described by

$$\begin{cases} \frac{d\widehat{V}_c}{dt} = -\frac{\widehat{V}_c}{R_0 C_0} + \frac{I}{C_0} + L_1(V_m - \widehat{V}) \\ \frac{d\widehat{SOC}}{dt} = -\frac{I}{C} + L_2(V_m - \widehat{V}) \end{cases} \quad (11)$$

Herein,  $V_m$  is the measured voltage of the battery,  $L_1$  and  $L_2$  are Kalman observer's gains. Therefore, error dynamics can be written as:

$$\begin{cases} \frac{d\widehat{V}_c}{dt} = -\frac{\widehat{V}_c}{R_0 C_0} + L_1(V_m - \widehat{V}) \\ \frac{d\widehat{SOC}}{dt} = L_2(V_m - \widehat{V}) \end{cases} \quad (12)$$

The observer gains, are selected such that the effect of both the process and measurement noises are suppressed and the error between the estimated and actual states of the system converge to zero irrespective of the initial conditions.

Here, we assume the SOC change of the battery is limited to the linear region (30-80%) where in the open circuit voltage of the battery,  $E_0$ , a linear function of SOC and body temperature. However, the design approach can be readily extended to the nonlinear SOC regions too. Under the above assumption, (2) can be rewritten in the following form:

$$E_0 = 3.49 + 0.09 SOC + 0.001T_{body} \quad (13)$$

$$V = E_0 - IR - V_c \quad (14)$$

$$V = 3.49 + 0.09 SOC + 0.001T_{body} - IR - V_c \quad (15)$$

As a result, both the estimated and the measured value of battery voltage can be written in the above form.

$$\begin{cases} V_m = E_0 - IR - V_c + \Delta V \\ \widehat{V} = \widehat{E}_0 - I_m R - \widehat{V}_c \end{cases} \quad (16)$$

therefore

$$\begin{cases} V_m = 3.49 + 0.09 (SOC + SOC_{bias}) + 0.001T_{body} - I_m R - V_c + \Delta V \\ \widehat{V} = 3.49 + 0.09 \widehat{SOC} + 0.001T_{body,m} - I_m \widehat{R} - \widehat{V}_c \end{cases} \quad (17)$$

$$\begin{aligned} R_1 &= V_m - \widehat{V} \\ R_1 &= 0.09\widehat{SOC} + 0.001\Delta T - \widehat{V}_c + \Delta V + K_{soc}SOC_{bias} \end{aligned} \quad (18)$$

where,

$$\begin{aligned} \widehat{SOC} &= SOC - \widehat{SOC} \\ \widehat{V}_c &= V_c - \widehat{V}_c \\ I_m &= I + \Delta I \\ T_{body,m} &= T_{body} + \Delta T \end{aligned} \quad (19)$$

where,  $R_1$  is the voltage residual,  $\Delta V$  is the fault in voltage sensor,  $\Delta T$  is the fault in temperature sensor,  $SOC_{bias}$  is the bias disturbance or fault on SOC,  $K_{soc}$  is a constant value,  $\widehat{R}$  is estimated value for R in the observer based on estimated SOC and measured temperature,  $I_m$  is measured current,  $T_{body,m}$  is measured temperature and  $\Delta I$  is fault in current sensor.

Since the Kalman filter gains are designed such that the estimation errors converge to zero, (18) can be rewritten as the following:

$$R_1 = K_{soc} SOC_{bias} + 0.001\Delta T + \Delta V \quad (20)$$

As it can be inferred from (20), the generated residual,  $R_1$ , is a function of  $SOC_{bias}$  which also covers the effect of current error, fault in voltage and temperature sensors in addition to effect of fault in current sensor. Hence, any faults in voltage, temperature, current sensor and bias disturbance in SOC will show up in  $R_1$ .

### E. Sliding Mode Observer

Nonlinear observers such as sliding mode observers can preserve the essential nonlinearity of the system and make the observer design process easier for systems with highly nonlinear dynamics. In this part, a nonlinear observer, based on sliding mode approach has been designed to detect the current sensor fault.

$$\begin{cases} m_c \frac{dT_{body}}{dt} = I^2(R + R_0) - hA_0 \left(1 + \frac{f_s}{2}\right) (T_{body} - T_{amb}) \\ m_c \frac{d\widehat{T}_{body}}{dt} = I_m^2(\widehat{R} + \widehat{R}_0) - hA_0 \left(1 + \frac{\widehat{f}_s}{2}\right) (\widehat{T}_{body} - T_{amb}) + \eta \end{cases} \quad (21)$$

Herein,  $\eta = K \cdot \text{sgn}(T_{body,m} - \widehat{T}_{body})$  and  $\text{sgn}(\cdot)$  is the sign function.

$$\begin{aligned} \text{Assuming} \\ I_m^2 &= I^2 + \delta I \end{aligned} \quad (22)$$

The error dynamics is described by (23):

$$\begin{aligned} m_c \frac{d\widehat{T}_{body}}{dt} &= \delta I (R + R_0 - \widehat{R} + \widehat{R}_0) - I^2(\widehat{R} + \widehat{R}_0) - \\ &hA_0 (\widehat{T}_{body}) - hA_0 \frac{\Delta f_s}{2} (\widehat{T}_{body} - T_{amb}) + \\ &K \cdot \text{sgn}(T_{body,m} - \widehat{T}_{body}) \end{aligned} \quad (23)$$

The sliding manifold is described as estimation error of the temperature of the battery:

$$S = e = T_{body} - \widehat{T}_{body} \quad (24)$$

The Lyapunov candidate, is chosen as (25), to analyze the stability of the observer error dynamics

$$V = \frac{1}{2} S^T S \quad (25)$$

$$\begin{aligned} \text{Then,} \\ \dot{V} &= S\dot{S} = e\dot{e} \end{aligned} \quad (26)$$

To have negative  $\dot{V}$  as sufficient condition for stability, the sliding mode's gain,  $K$ , is selected large enough to satisfy the constraint.

$$\text{if } K > \left| \frac{(R+R_0)}{mc} \right| \text{ then } \dot{V} < 0 \quad (27)$$

Herein,  $R$  and  $R_0$  can be considered with their maximum possible values.

On the sliding manifold  $S = 0$ ,

$$\begin{aligned} \tilde{T}_{body} &= 0 \text{ and } \frac{d\tilde{T}_{body}}{dt} = 0 \\ \eta &= K \cdot \text{sgn}(\tilde{T}_{body}) \end{aligned} \quad (28)$$

On the sliding manifold, the equivalent control of the sliding mode can be extracted with a low pass filter as:

$$R_2 = \text{filter} \left[ \frac{m \cdot c}{(R+R_0)} K \cdot \text{sgn}(\tilde{T}_{body}) \right] \quad (29)$$

As it can be inferred from (29), the current sensor fault along with the faults in the temperature sensor and fan's actuator fault will show up in the generated residual,  $R_2$ .

In the next step, using the estimated temperature via sliding mode observer and the measured battery temperature, the third residual,  $R_3$  will be generated.

$$R_3 = T_{body,m} - \hat{T}_{body} \quad (30)$$

Since the estimation error of battery temperature in the sliding manifold converges to zero,  $R_3$  will show failure and faults in the battery system, which cause to changes in battery temperature dynamics. As a result, failure in the fan and fault in temperature sensor will show up in  $R_3$ .

In the next section, based on probability density analysis for each of these residuals, a threshold will be set to generate a fault signature.

## THRESHOLD SETTING

The generated residuals can be evaluated based on selected thresholds. Various methods for threshold setting have been addressed in different studies [10], [19]. In this paper, probability density analysis has been used for each residual to find optimum thresholds such that the probabilities of false alarms and of misdetection have their minimum possible values.

To set a threshold, for each residual, probability densities for both faulty and non-faulty data of the residuals are plotted as in Fig 2. The intersection of the plots shows the optimum value of the threshold. The plot depicts the probability density of the voltage residual ( $R_1$ ). The probability density analysis has been similarly used for the current residual ( $R_2$ ) and the temperature residual ( $R_3$ ).

It can be demonstrated from Fig. 2 that, a fault in the battery system changes the mean and standard deviation of normal data's probability density. So, in all three cases, thresholds can be selected based on means and standard deviations in the fault-free cases. Hence, thresholds for voltage and current residuals,  $R_1$  and

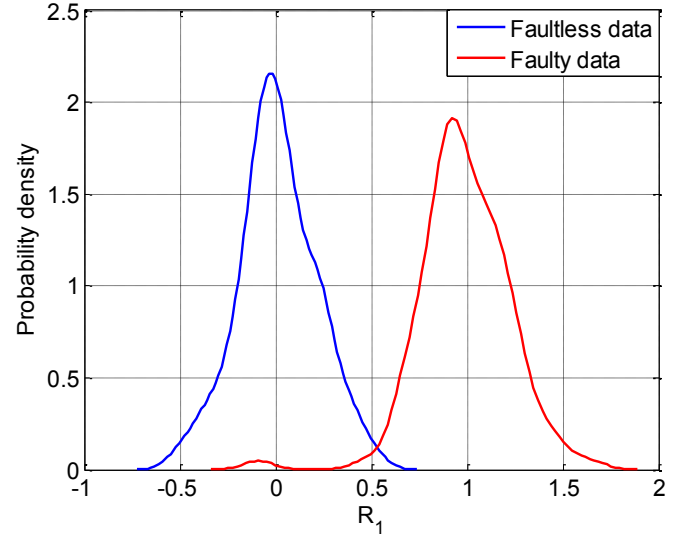


**Figure 2:** Probability density analysis of voltage residual

$R_2$ , have been selected as  $\gamma_1 = \mu_1 + 1.1\sigma_1$  and  $\gamma_2 = \mu_2 + 4.4\sigma_2$  respectively.

These thresholds are sensitive to fault detection while the probabilities of false alarms are small too. Also, for the last residual,  $R_3$  which is temperature residual, the threshold is selected as  $\gamma_3 = \mu_3 + 1.1\sigma_3$  based on the probability analysis. Whenever one of these residuals surpasses its own threshold, a fault detection signal will be triggered to declare that a fault is detected in the system.

$$|R_i| > \gamma_i \quad (31)$$

Fault isolation is not the same as fault detection in a system. Indeed, in order to isolate a fault in a system a unique signature based on all available residuals in the system, is required. By considering designed thresholds for residuals, fault signature can be derived and evaluated as in Table 1. It can be demonstrated that, all faults, failure and disturbance in the system have their own unique signature. Hence, in case of individual fault scenario in the battery, detection and isolation of the faults can be guaranteed based on the three residuals and the signature table.

**Table 1.** Faults signature table

Fault \ Residual	SOC bias	Voltage sensor fault	Fan actuator	Current sensor fault	Body temp fault
$R_1$	1	1	0	0	1
$R_2$	1	0	1	1	1
$R_3$	0	0	1	0	1

## RESULTS & DISCUSSIONS

In this section, numerical simulation results in single fault scenario are discussed. In order to simulate and analyze possible faults in a realistic scenario, we used experimental set of data for the applied current to the battery. Also, a white Gaussian noise is added as measurement noise to each measured output.

To simulate the sensors faults, a 1 v bias voltage on voltage sensor at  $t = 1500\text{sec}$  and a  $1^\circ\text{C}$  bias fault on body temperature sensor at  $t = 2900\text{sec}$  have been considered. Also, a gain fault on current sensor is injected at  $t = 2500\text{sec}$ . Cooling fan actuator's failure is simulated as actuator fault at  $t = 2000\text{sec}$ . The failure and each of sensor faults lasts for  $100\text{sec}$  in the system. In addition, the effect of disturbance in SOC, is simulated with a trapezoid form of the disturbance starting at  $t = 1000\text{sec}$  and ending at  $t = 1120\text{sec}$ . Fig.3 shows all mentioned faults in the system. All available measurements containing current, voltage and body temperature in presence of the faults are depicted in Fig.4.

Fig.5 illustrates the residuals while faults and SOC disturbance occur in the system. Each fault can affect one or more residuals as it is discussed in Section III. Failure in fan actuator, faults in voltage and body temperature sensors will affect the voltage residual  $R_1$ . Once one of these faults occurs in the system,  $R_1$  will exceed the threshold  $\gamma_1$  and will trigger the

fault detection signal. As it can be inferred, the bias in SOC, fan actuator's failure and faults in current and body temperature sensors have appeared in  $R_2$ . In a similar case, Fig.5 clarifies that the residual  $R_3$  is sensible to fan actuator's failure and the fault in body temperature sensor. Since the temperature dynamics of the battery is slow, the effect of the failure in the fan will last more than 100 secs in the system and this effect can be seen in  $R_2$  and  $R_3$ .

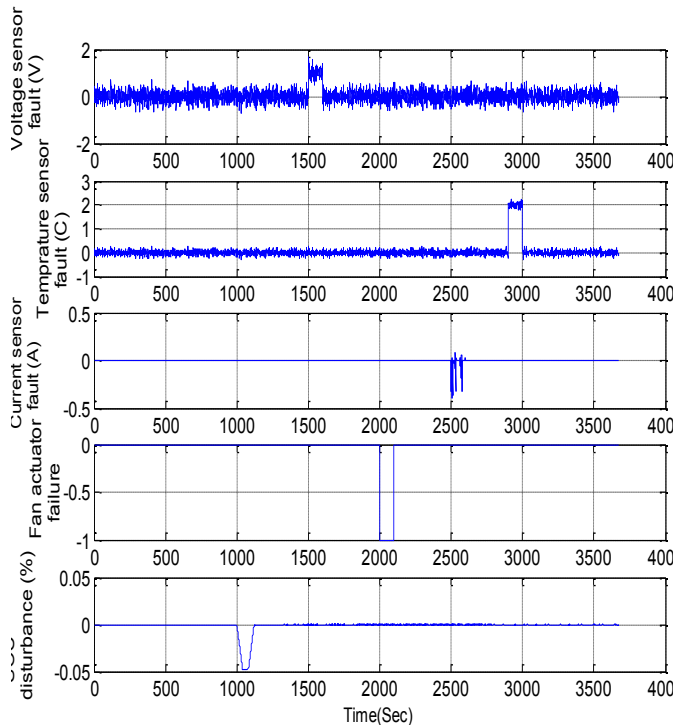


Figure 3: Possible faults and failures injected in battery's system

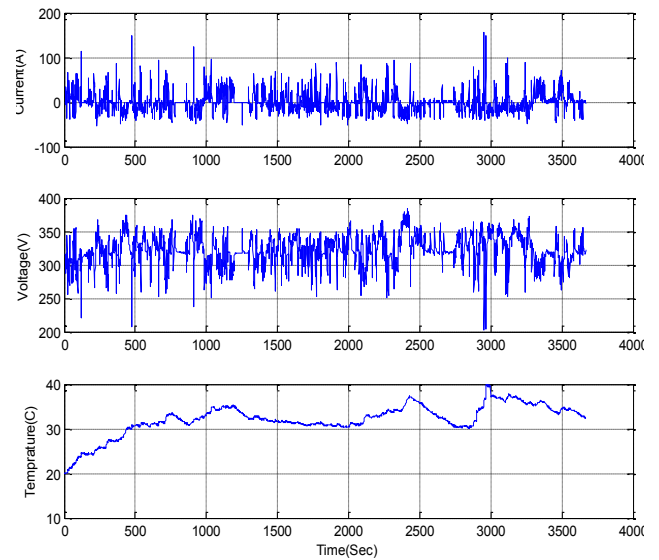


Figure 4: Measureable input and outputs of the battery

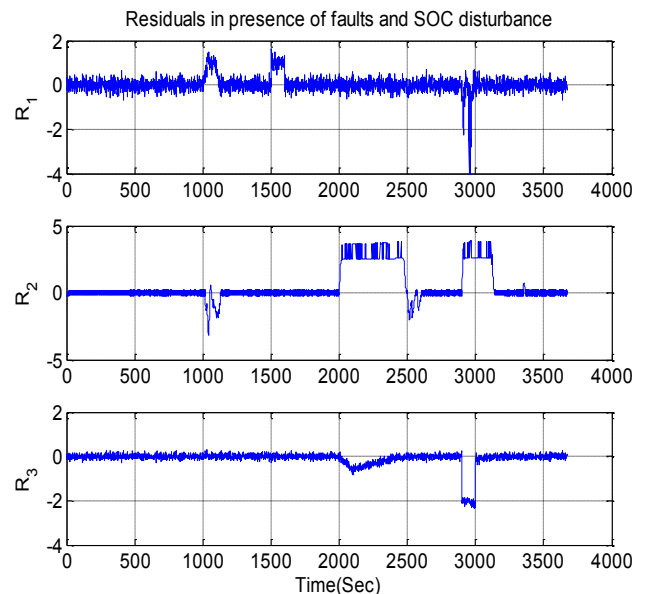
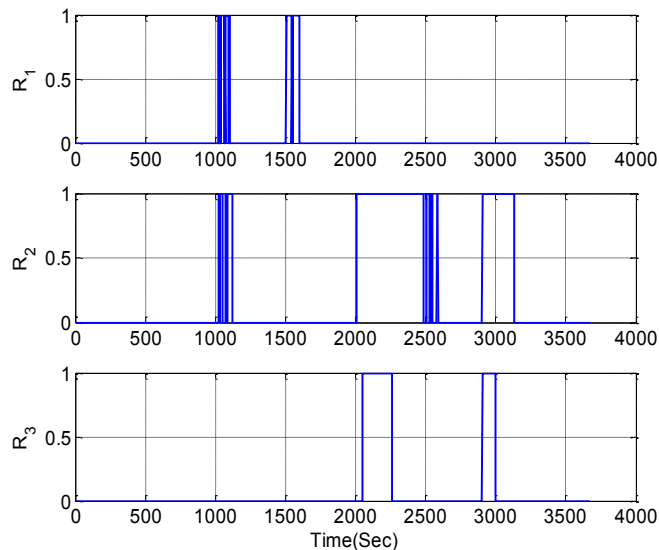


Figure 5: Residuals in the presence of faults and SOC disturbance



**Figure 6:** Residuals signature in the presence of faults and SOC disturbance

As a conclusion, fault in voltage sensor appears only in  $R_1$  and fault in current sensor affects only  $R_2$ , while faults in temperature sensor can be seen in all residuals. Also, failure in fan actuator changes the value of  $R_2$  and  $R_3$  while, disturbance in SOC changes  $R_1$  and  $R_2$ . Hence, each fault or failure in the battery system has its own specific fault signature as presented in Table 1, which helps to detect and isolate the specific fault in the battery. The faults signatures are plotted in Fig.6

## CONCLUSION

In this paper, an observer-based diagnosis scheme has been proposed and demonstrated to detect and isolate these faults in the battery system. Both sliding mode and Kalman filter theories are used to design separate observers in the diagnosis scheme. The designed observers generate three residuals which can be affected via different faults and failures as well as SOC bias. In order to isolate these abnormalities in the battery, thresholds are set for residuals to map each fault to a specific fault signature. Using the derived signature, it is demonstrated that five different types of faults, including current, temperature and voltage sensor, cooling fan actuator and SOC bias faults can be distinguished and isolated from each other.

## REFERENCES

[1] X. Tang, X. Mao, J. Lin, and B. Koch, "Capacity Estimation for Li-ion Batteries", *American Control Conference*, pp. 947- 952, 2011.

[2] B. S. Bhangu, P. Bentley, D. A. Stone, and C. M. Bingham, "Nonlinear observers for predicting state-of-charge and state-of-health of Lead-Acid batteries for hybrid-electric vehicles," *IEEE Transactions on Vehicular Technology*, vol. 54, pp. 783–794, 2005.

[3] Linden, David, and Thomas B. Reddy. "Handbook of batteries", *New York*.

[4] P. Arora, R. E. White, and M. Doyle, "Capacity fade mechanisms and side reactions in lithium-ion batteries," *Journal of Electrochemical Society*, vol. 145, Issue. 10, pp. 3647–3667, 1998.

[5] D. Aurbach, E. Zinigrad, Y. Cohen, and H. Teller, "A short review of failure mechanisms of lithium metal and lithiated graphite anodes in liquid electrolyte solutions," *Solid State Ionics*, vol. 148, pp. 405–416, 2002.

[6] T. Zining, F. Yunzhou, and P. Qingfeng, "A LabVIEW-based fault diagnosis system for lithium-ion battery", *Asia-Pacific Power and Energy Engineering Conference*, pp. 1-4, 2011.

[7] J. Zhang, and J. Lee, "A review on prognostics and health monitoring of Li-ion battery", *Journal of Power Sources*, vol. 196, Issue. 15, pp. 6007 – 6014, 2011.

[8] J. Marcicki, S. Onori, and G. Rizzoni, "Nonlinear fault detection and isolation for a lithium-ion battery management system", *Dynamic Systems and Control Conference*, pp. 607-614, 2010.

[9] S. Dey, and B. Ayalew, "A Diagnostic Scheme for Detection, Isolation and Estimation of Electrochemical Faults in Lithium-ion Cells", *accepted in ASME 2015 Dynamic System and Control Conference*, Columbus, OH, October 2015.

[10] G. Ablay, "An Observer-Based Fault Diagnosis in Battery Systems of Hybrid Vehicles", *8th International Conference on Electrical and Electronics Engineering (ELECO)*, pp. 238 – 242, 2013.

[11] L. Liu, J. Park, X. Lin, A. M. Sastry, and W. Lu, "A thermal-electrochemical model that gives spatial-dependent growth of solid electrolyte interphase in a Li-ion battery", *Journal of Power Sources*, vol. 268, pp. 482 – 490, 2014.

[12] T. F. Fuller, M. Doyle, and J. Newman, "Simulation and optimization of the dual lithium ion insertion cell," *Journal of the Electrochemical Society*, vol. 141, no. 1, pp. 1-10, 1994.

[13] K. A. Smith, C. D. Rahn, and C. Wang, "Model-based electrochemical estimation of lithium-ion batteries," in *IEEE 2008 International Conference on Control Applications*, pp. 714-719, 2008.

[14] X. Hu, S. Li, and H. Peng, "A comparative study of equivalent circuit models for Li-ion batteries", *Journal of Power Sources*, vol. 198, pp. 359 – 367, 2012.

[15] I.-S. Kim, "The novel state of charge estimation method for lithium battery using sliding mode observer," *Journal of Power Sources*, vol. 163, no. 1, pp. 584–590, 2006.

[16] Y. Hu and S. Yurkovich, "Battery cell state-of-charge estimation using linear parameter varying system techniques," *Journal of Power Sources*, vol. 198, pp. 338–350, 2012.

[17] Saha, B., Goebel, K., Poll, S., and Christophersen, J., "An integrated approach to battery health monitoring using

bayesian regression and state estimation”. *IEEE Autotestcon*, pp. 646-653, 2007.

[18] Ng, K. S., Moo, C., Chen, Y., and Hsieh, Y, “Enhanced coulomb counting method for estimating state-of-charge and state-of-health of lithium-ion batteries”. *Applied Energy*, vol. 86, no. 9, pp. 1506-1511, 2009.

[19] A. Hashemi, P. Pisu, “Adaptive Threshold-Based Fault Detection and Isolation for Automotive Electrical Systems”, *9th World Congress on Intelligent Control and Automation*, , pp. 1013 – 1018, 2011.